First Stage of Oxygen Aggregation in Silicon: The Oxygen Dimer

S. Öberg

Department of Mathematics, University of Luleå, Luleå, S97187, Sweden

C. P. Ewels and R. Jones

Department of Physics, University of Exeter, Exeter, EX4 4QL, United Kingdom

T. Hallberg and J. L. Lindström

Department of Physics and Measurement Technology, Linköping University, S-581 83 Linköping, Sweden

L. I. Murin

Institute of Solid State and Semiconductor Physics, Minsk 220072, Belarus

P. R. Briddon

Department of Physics, University of Newcastle upon Tyne, Newcastle, NE1 7RU, United Kingdom

The structure and dynamic properties of the interstitial oxygen dimer in silicon are found using a combination of infrared spectroscopy and *ab initio* modeling. We find that the stable dimer consists of a pair of inequivalent weakly coupled interstitial oxygen atoms separated by a Si-Si bond. Two high frequency modes are decoupled in one ^{16}O-^{18}O combination but are strongly mixed in the other combination. A third lower lying mode involves the compression of the Si-Si bond joining the oxygen atoms and gives distinct modes in the mixed ^{16}O-^{18}O case.   [S0031-9007(98)07293-7]

When Si containing oxygen is annealed at temperatures below 550 °C, a family of electrically active thermal double donor, TDD(N), defects containing oxygen is formed [1,2]. In spite of intense efforts for over forty years, there is currently no consensus on their structure or the processes involved in their creation [3]. It is believed that the defects are formed sequentially by an activated process in which TDD(N) is transformed into TDD($N + 1$) by the addition of an oxygen species. The activation energies for the rate of TDD(N) → TDD($N +$ 1) lie around 1.7 ± 0.2 eV [4,5] and are much lower than the migration energy of interstitial oxygen (O_i): about 2.54 eV. It has long been suggested that this anomalous growth is due to a rapidly diffusing interstitial oxygen dimer (O_{2i}) [6,7] although the evidence for this is circumstantial. O_{2i} is then regarded as a precursor for the thermal donors and thus there is a great deal of interest in its properties. This paper, through a combination of experimental vibrational mode studies and theoretical modeling, presents a unique model for its structure.

Experimental evidence for O_{2i} has come from previous infrared (IR) absorption measurements where the integrated absorption intensities (IA) of two local modes at 1012 and 1060 cm^{-1} were found to be proportional to the square of the oxygen concentration [8,9]. However, a surprising result was that additional modes were not detected in material containing ^{16}O-^{18}O [10]. This conflicts with previous theoretical modeling which has suggested that a dimer, capable of diffusing rapidly, consists of two neighboring O_i defects [11–14]. We show here, how-

ever, that there are unique modes due to the dimer in material containing ^{16}O-^{18}O but these modes imply that the oxygen atoms are separated by a Si-Si bond. This then raises the question as to whether the dimer can diffuse rapidly.

The experimental investigation used three types of samples. The first (a) contained ^{16}O, while the second (b) contained mainly ^{18}O. The third (c) contained equal concentrations of ^{16}O and ^{18}O. Samples (a) were fabricated from commercially grown phosphorus doped Cz-silicon with a resistivity of about 50 Ω cm and oxygen and carbon concentrations in the range $(10-14) \times 10^{17}$ cm^{-3} and $(0.5-5) \times 10^{16}$ cm^{-3}, respectively. Samples (b) and (c) consisted of float-zone Si material and were isotopically enriched with ^{18}O$_i$. In (b) the concentrations of ^{16}O$_i$ and ^{18}O$_i$ were 6×10^{16} cm^{-3} and $(12-18) \times 10^{17}$ cm^{-3}, respectively, while (c) contained about 10^{18} cm^{-3} of each oxygen isotope. The carbon concentration in samples (b) and (c) was about $(2-4) \times 10^{16}$ cm^{-3} and their resistivities were about 100 Ω cm. The measurements were performed at room temperature (295 K) and at 10 K, to a spectral resolution of 1 and 0.5 cm^{-1}, respectively, using a Bruker IFS 113v Fourier transform infrared spectrometer. The concentrations of ^{16}O$_i$, ^{18}O$_i$, and C$_s$ were monitored by measuring the intensities of the 1107 (^{16}O$_i$) [15], 1058 (^{18}O$_i$), and 605 cm^{-1} [16] absorption bands. In order to increase the intensity of the rather weak dimer related vibrational modes in the as-grown material, the samples were electron irradiated at about 350 °C, using 2 MeV e-irradiation.
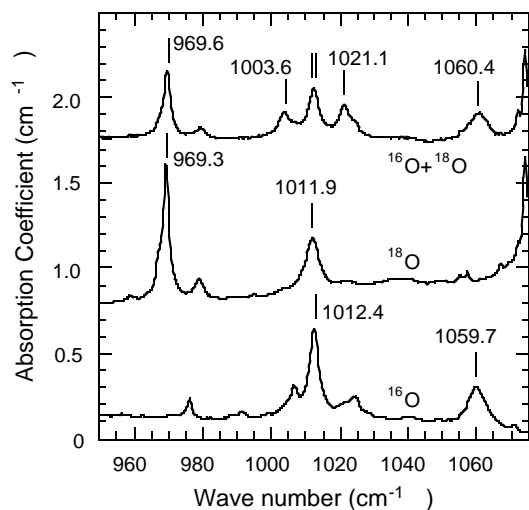
FIG. 1. Absorption spectra of the two highest oxygen dimer modes for ^{16}O, ^{18}O, and $^{16}O + {}^{18}O$ samples.

This increased their intensities by about an order of magnitude compared with as-grown material [10].

    The experimental results are shown in Figs. 1, 2, and 3 for (a) ^{16}O, (b) ^{18}O, and (c) $^{16}O + {}^{18}O$ samples. For material (a) or (b) containing only ^{16}O and ^{18}O, these figures show four dimer related IR vibrational bands positioned at about 1060, 1012, 690, and 556 cm^{-1} for (a), and 1012, 969, 680, and 556 cm^{-1} for material (b), in agreement with previous studies [8,10]. However, the spectrum for the mixed-isotopic sample (c) shown in Fig. 1 has not been reported previously. This spectrum shows that additional dimer bands occur at 1003.6 and 1021.1 cm^{-1}. These represent coupled modes and they prove that the defect contains at least two coupled O atoms. We have found that the strength of these bands correlates with those of the other dimer related modes and they have the same very special temperature dependence as the 1060 and 1012 cm^{-1} modes [8]. That is, their positions increase by some 0.5–1.5 cm^{-1} when the temperature is increased from 10 K to room temperature. These shifts are unusual and opposite to what is usually encountered. The ratios of the IA intensities of the 1060, 1021, 1012, 1004, and 969 cm^{-1} modes in the mixed $^{16}O + {}^{18}O$ case are approximately 2:1:2:1:2, respectively. Thus the intensities of the mixed modes at 1004 and 1021 cm^{-1} are one-half those of the ^{16}O-^{16}O and ^{18}O-^{18}O bands. Normally, a mixed mode between equivalent oscillators would be expected to be twice as intense as the other bands. This follows as the number of ^{16}O-^{18}O defects is twice that of ^{16}O-^{16}O or ^{18}O-^{18}O in samples such as (c) which contains equal amounts of ^{16}O and ^{18}O. These unusual ratios will be explained below.

    Figure 2 shows a broadband due to a coupled motion of the oxygen atoms also occurs at 685.7 cm^{-1} (^{16}O-^{18}O) as this is related to modes at 690 (^{16}O-^{16}O) and 680 cm^{-1} (^{18}O-^{18}O). The ratios of the IA intensities of the 690, 686, and 680 bands are 1:2:1. Figure 3 shows that the

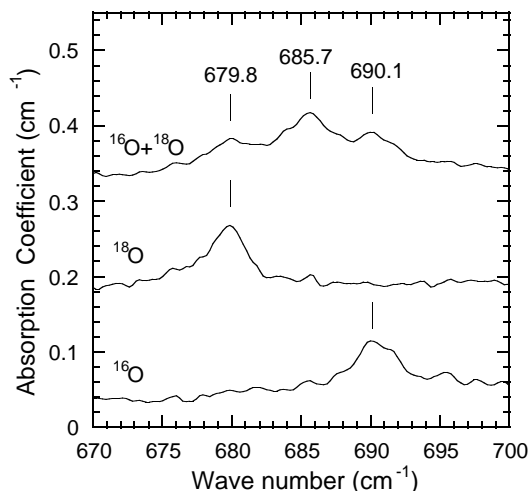556 cm^{-1} mode, whose intensity is correlated with the other dimer bands, is Si related as it shifts only slightly with the oxygen isotopic mass.

    The theoretical analysis was performed with an *ab initio* modeling program (AIMPRO), based on density functional theory and utilizing large 88-atom H-terminated clusters containing pairs of oxygen atoms. The method [17] has been used previously to explore the structure and vibrational modes of VO_n defects [18] and shallow thermal donors [19] as well as oxygen dimers [13]. The basis was similar to that used previously, except additional bond centered basis functions were placed between second shell neighboring Si atoms within the defect core.

    We first note that the two frequencies at 1012 and 1060 cm^{-1} are close to that of interstitial oxygen, suggesting that the oxygen atoms are close to their normal bond centered sites. This suggests that the dimer consists of a pair of interstitial oxygen atoms and refutes the old
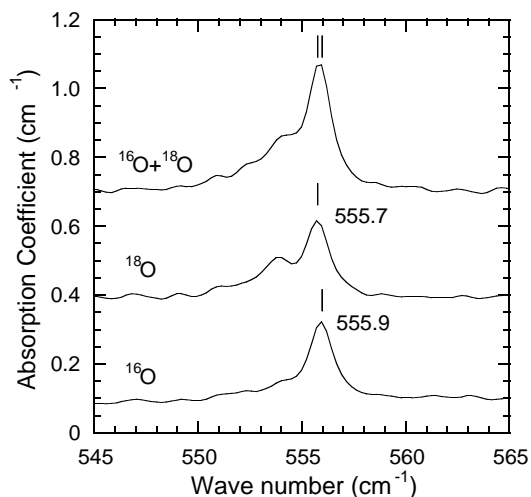

FIG. 2. Absorption spectra of the third oxygen dimer mode for ^{16}O, ^{18}O, and $^{16}O + {}^{18}O$ samples.

FIG. 3. Absorption spectra of the lowest frequency oxygen dimer mode for ^{16}O, ^{18}O, and $^{16}O + {}^{18}O$ samples.
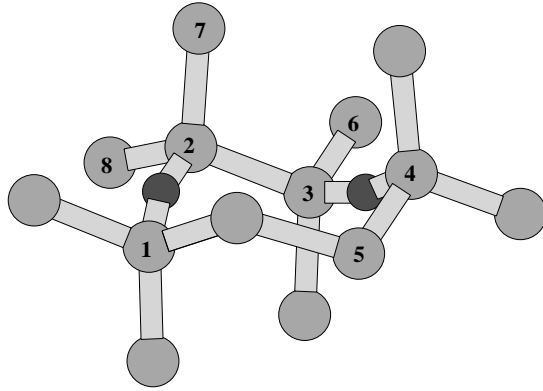
FIG. 4. The stable oxygen dimer. The two oxygen atoms have slightly different Si-O bond lengths and are inequivalent (see text).

idea, based on volumetric considerations, that aggregation of two O_i defects necessarily kicks out a Si interstitial. Furthermore, the distinct modes detected in the isotopically mixed samples imply that the O atoms are close together. This suggests three possibilities: (i) when the O atoms lie at neighboring bond center sites (2—3, 3—4 in Fig. 4), (ii) when they are separated by a Si-Si bond and lie in parallel Si-Si bonds (8—2, 3—4 in Fig. 4), and (iii) when they are separated by a Si-Si bond but lie in skewed Si-Si bonds (1—2, 3—4 in Fig. 4). More distant dimers analyzed in a larger cluster possessed decoupled modes. It is found that the third cluster has the lowest energy but the energy difference with the first is not significant. Structure (i), in which the oxygen atoms lie at neighboring bond centered sites, has an energy only 0.14 eV greater than (iii) while the energy of (ii) is greater by 1.3 eV. The actual energy differences are dependent on the distribution and number of bond centers. However, we show below that the calculated vibrational modes of structure (i) are inconsistent with the experimental values.

It seems that the stability of structure (iii) comes from a partial cancellation of the long range compressive strain field of one oxygen atom by the other. The O atom between 1 and 2 in Fig. 4 gives a compressive strain field

in the (011) plane occupied by atoms 1, 2, and 7 and a tensile strain field in the ($0\bar{1}1$) plane occupied by 2, 3, 4, and the second O atom. It is important to note that the two O atoms are not equivalent and there are small differences in the Si-O bond lengths and angles. The O atom bonded to 3 has a slightly shorter bond (1.617 Å) than with atom 4 (1.640 Å) while the O atom between 1 and 2 has a shorter bond (1.622 Å) with 1 rather than 2 (1.647 Å). The Si-O-Si bond angles are very close to 166°. The defect does not possess any deep electronic gap levels.

The dynamical matrix for the cluster was then constructed from the *ab initio* second derivatives of the energy between the two O atoms and their Si neighbors along with ones between more remote atoms found from a Musgrave-Pople potential given previously [20]. The vibrational modes of the dimer are then found from the dynamical matrix and are given in Table I.

The calculated frequencies lie within 55 cm^{-1} of the observed modes and this error is typical of the method. The two upper modes, at 1085 and 1036 cm^{-1}, are due to an asymmetric stretch of the O atom with the shorter (i.e., between 3 and 4 in Fig. 4) and longer (i.e., between 1 and 2) bonds, respectively. This follows as the 1085 cm^{-1} mode shifts by only 3 cm^{-1} when the ^{16}O atom between 1 and 2 is replaced by ^{18}O, while the 1036 cm^{-1} mode shifts by 44 cm^{-1}. These shifts are in very good agreement with the observed ones of ~0 and 43 cm^{-1}. The difference of 50 cm^{-1} between the two modes agrees well with the observed difference of 45 cm^{-1} and primarily arises from the inequivalence in the local structure around each O atom. In the ^{18}O-^{18}O case, the two highest modes are shifted by ~47 cm^{-1}, respectively, in reasonable agreement with the observed shifts of 48 and 43 cm^{-1}.

Replacing the second oxygen atom between 3 and 4 by ^{18}O might be expected to reduce the 1085 cm^{-1} mode to 1038 cm^{-1}. However, this frequency is almost degenerate with the mode of the first ^{16}O atom. In this case the coupling between the two O atoms becomes very important and mixed modes at 1053 and 1020 cm^{-1}

TABLE I. Calculated and observed local vibrational modes for the oxygen dimer (cm^{-1}). Bracketed value shows downwards shift of the mode from the ^{16}O-^{16}O case. The last column gives the frequencies when the two Si atoms connecting the dimer are replaced by ^{29}Si. ND: not detected.

^{16}O-^{16}O	^{18}O-^{16}O	^{16}O-^{18}O	^{18}O-^{18}O	^{29}Si^{16}O-^{16}O
Calculated				
1084.9	1082.2 (2.7)	1053.2 (31.7)	1038.1 (46.8)	1080.8 (4.2)
1035.7	991.4 (44.3)	1020.2 (15.5)	988.3 (47.4)	1032.8 (2.9)
636.6	634.2 (2.5)	627.3 (9.3)	624.6 (12.1)	630.6 (6.0)
580.7	579.4 (1.4)	578.2 (2.5)	577.0 (3.8)	574.8 (5.9)
574.1	569.8 (4.3)	573.9 (0.1)	569.4 (4.7)	570.6 (3.4)
Observed				
1059.7	~1060 (ND)	1021.1 (38.6)	1011.9 (47.8)	
1012.4	969.6 (42.8)	1003.6 (8.8)	969.3 (43.1)	
690.1	685.7 (4.4)	~685.7 (~4.4)	679.8 (10.3)	
555.9	~555.8 (ND)	~555.8 (ND)	555.7 (0.2)	

are found. The 32 and 16 cm^{-1} drop in the frequencies from the ^{16}O-^{16}O case are in fair agreement with the experimental shifts of 39 and 9 cm^{-1}.

We can now understand the observed 2:1:2:1:2 ratio of the intensities of the modes. From Table I we see that the mode at about 1085 cm^{-1} occurs twice: once for ^{16}O-^{16}O and once for ^{18}O-^{16}O. Modes around 1053 cm^{-1} occur with one combination of isotopes: ^{16}O-^{18}O, whereas there are two combinations giving modes at about 1036 cm^{-1} (^{16}O-^{16}O, ^{18}O-^{18}O). Finally, there is one combination giving a mode at 1020 cm^{-1} (^{16}O-^{18}O) and two at about 991 cm^{-1} (^{18}O-^{16}O, ^{18}O-^{18}O). Thus the observed ratios of the intensities of these modes can be explained if they all possess the same oscillator strength.

The 637 cm^{-1} mode is due to the movement of both O atoms perpendicular to the Si-O bonds and involves a substantial displacement of atoms 1 and 2. This mode shifts 3 and 9 cm^{-1} in the mixed case and 12 cm^{-1} in the ^{18}O-^{18}O case. These are to be compared with a broadband shifted by ∼5 cm^{-1}, in the mixed case, and 10 cm^{-1} for ^{18}O-^{18}O. There are two lower modes which have small shifts of about 4 cm^{-1} with ^{18}O.

The 637 and 581 cm^{-1} modes involve a stretch of the central Si-Si bond which has been compressed by the adjacent oxygen atoms as they shift by ∼6.0 cm^{-1} when the two Si atoms of the bond connecting the two O atoms are replaced with ^{29}Si.

The dimer structure (iii) is not consistent with previous calculations which favored structure (i) [11–14]. As the O atoms are at neighboring bond centers in this structure, the two highest modes are strongly coupled. We found them to lie at 926 and 1101 cm^{-1} (^{16}O-^{16}O), and these shift to 907 and 1072 cm^{-1} (^{18}O-^{16}O) and to 895 and 1087 cm^{-1} (^{16}O-^{18}O). The fact that both modes shift substantially when either oxygen atom is replaced by ^{18}O conflicts with the experimental observations, and this model can be discounted. It seems that the resulting lattice strain prevents the two oxygen atoms from sharing neighboring bond center sites. Nevertheless, the energy difference between structures (iii) and (i) is quite small ∼0.1 eV. This suggests that there are two types of dimers: those of type (i) would be in the minority but would be able to diffuse quickly, and the common (iii) variety whose migration energy is unknown.

In conclusion, we have investigated the vibrational modes of the oxygen dimer in silicon using ^{16}O-^{18}O mixtures and demonstrated that additional modes are present, proving that these vibrational bands are associated with at least two coupled oxygen atoms. *Ab initio* modeling has shown that the dimer consists of two bond centered oxygen defects separated by a Si-Si bond and lying in skewed ⟨111⟩ bonds. This structure has modes in close agreement with the observed modes. The defect is only slightly more stable than a pair of oxygen atoms at neighboring sites. Finally, we note that the combination of infrared absorp-

tion experiments on mixed isotopic specimens combined with *ab initio* modeling provides a powerful tool for the identification of defects.

[1] C. S. Fuller, J. A. Ditzenberger, N. B. Hannay, and E. Buehler, Phys. Rev. **96**, 833 (1954).

[2] W. Kaiser, H. L. Frisch, and H. Reiss, Phys. Rev. **38**, 1546 (1958).

[3] The proceedings of a recent conference discussing the thermal donor problem is *Early Stages of Oxygen Precipitation in Silicon,* edited by R. Jones, NATO ASI Series (3. High Technology), Vol. 17 (Kluwer, Dordrecht, 1996).

[4] V. P. Markevich, L. F. Makarenko, and L. I. Murin, Phys. Status Solidi A **97**, 173 (1983).

[5] M. Claybourn and R. C. Newman, Appl. Phys. Lett. **51**, 2197 (1987).

[6] U. Gösele and T. Y. Tan, Appl. Phys. A **28**, 79 (1982).

[7] S. A. McQuaid, M. J. Binns, C. A. Londos, J. H. Tucker, A. R. Brown, and R. C. Newman, J. Appl. Phys. **77**, 1427 (1995).

[8] T. Hallberg, J. L. Lindström, L. I. Murin, and V. P. Markevich, Mater. Sci. Forum **258–263**, 361 (1997).

[9] L. I. Murin, T. Hallberg, V. P. Markevich, and J. L. Lindström, Phys. Rev. Lett. **80**, 93 (1998).

[10] J. L. Lindström, T. Hallberg, D. Åberg, B. G. Svensson, L. I. Murin, and V. P. Markevich, Mater. Sci. Forum **258–263**, 367 (1997).

[11] L. C. Snyder, J. W. Corbett, P. Deák, and R. Wu, Mater. Res. Soc. Symp. Proc. **104**, 179 (1988).

[12] M. Needels, J. D. Joannopoulos, Y. Bar-Yam, and S. T. Pantelides, Phys. Rev. B **43**, 4208 (1991); Mater. Res. Soc. Symp. Proc. **209**, 103 (1991).

[13] C. P. Ewels, R. Jones, and S. Öberg, *Early Stages of Oxygen Precipitation in Silicon,* edited by R. Jones, NATO ASI Series (3. High Technology), Vol. 17 (Kluwer, Dordrecht, 1996), p. 141.

[14] D. J. Chadi, Phys. Rev. Lett. **77**, 861 (1996).

[15] A. Baghdadi, W. M. Bullis, M. C. Croarkin, Y.-Z. Li, R. I. Scace, R. W. Series, P. Stallhofer, and M. Watanabe, J. Electrochem. Soc. **136**, 2015 (1989).

[16] *ASTM Book of Standards,* Test Method for Substitutional Carbon Atoms of Silicon by Infrared Absorption, F123-86 (American Society for Testing and Materials, Philadelphia, 1986), p. 252.

[17] R. Jones, and P. R. Briddon, in *Identification of Defects in Semiconductors,* edited by M. Stavola, Semiconductors and Semimetals Series Vol. 51A (Academic Press, Boston, 1998), Chap. 6, p. 287.

[18] C. P. Ewels, R. Jones, and S. Öberg, Mater. Sci. Forum **196**, 1297 (1995).

[19] C. P. Ewels, R. Jones, S. Öberg, J. Miro, and P. Deák, Phys. Rev. Lett. **77**, 865 (1996).

[20] R. Jones, J. Phys. C **20**, L271 (1987).